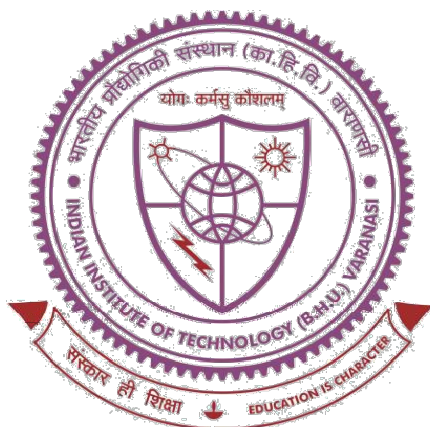


**PREPARATION, PHYTOCHEMICAL INVESTIGATION AND  
EVALUATION OF ANTI-DIABETIC ACTIVITY OF  
POLYHERBAL EXTRACT**



**Thesis submitted in partial fulfilment for the  
Award of Degree**

**Doctor of Philosophy**

**By**

**Amit Kumar Singh**

**DEPARTMENT OF PHARMACEUTICAL ENGINEERING & TECHNOLOGY  
INDIAN INSTITUTE OF TECHNOLOGY  
(BANARAS HINDU UNIVERSITY)  
VARANASI – 221005  
INDIA**

**Roll No- 18161516**

**Year 2024**



**DEPARTMENT OF PHARMACEUTICAL  
ENGINEERING & TECHNOLOGY INDIAN  
INSTITUTE OF TECHNOLOGY (B. H. U.)  
VARANASI – 221005 INDIA**

---

**CERTIFICATE**

It is certified that the work contained in the thesis titled "*Preparation, phytochemical investigation and evaluation of anti-diabetic activity of polyherbal extract*" by *Mr. Amit Kumar Singh* has been carried out under my supervision and that this work has not been submitted elsewhere for a degree.

It is further certified that the student has fulfilled all the requirements of Comprehensive Examination, Candidacy and SOTA for the award of Ph.D. degree.

**Dr. Sunil Kumar Mishra**

Supervisor

*Dr. S. K. Mishra*

सहायक-आचार्य / Assistant Professor  
भैषजकीय अभियांत्रिकी एवं प्रौद्योगिकी विभाग /  
Department of Pharmaceutical Engineering & Technology  
भारतीय प्रौद्योगिकी संस्थान / INDIAN INSTITUTE OF TECHNOLOGY  
(बनारस हिन्दू विश्वविद्यालय) / (BANARAS HINDU UNIVERSITY)  
वाराणसी-२२१००५ / Varanasi-221005



**DEPARTMENT OF PHARMACEUTICAL  
ENGINEERING & TECHNOLOGY INDIAN  
INSTITUTE OF TECHNOLOGY (B. H. U.)  
VARANASI – 221005 INDIA**

**DECLARATION BY THE CANDIDATE**

I, "**Amit Kumar Singh**", certify that the work embodied in this thesis is my own bonafide work and carried out by me under the supervision of "**Dr. Sunil Kumar Mishra**" from "**January 2019**" to "**March 2024**", at the "**Department of Pharmaceutical Engineering & Technology**", **Indian Institute of Technology (BHU)**, Varanasi. The matter embodied in this thesis has not been submitted for the award of any other degree/diploma. I declare that I have faithfully acknowledged and given credits to the research workers wherever their works have been cited in my work in this thesis. I further declare that I have not willfully copied any other's work, paragraphs, text, data, results, etc., reported in journals, books, magazines, reports dissertations, theses, etc., or available at websites and have not included them in this thesis and have not cited as my own work.

Date:

Place: Varanasi

**Amit Kumar Singh**

**CERTIFICATE BY THE SUPERVISOR**

It is certified that the above statement made by the student is correct to the best of my knowledge.

**Dr. Sunil Kumar Mishra**

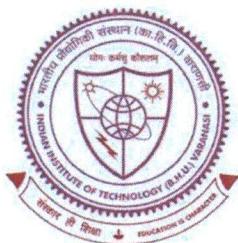
**Supervisor**

सहायक-आचार्य / Assistant Professor  
भैषजकीय अभियांत्रिकी एवं प्रौद्योगिकी विभाग /  
Department of Pharmaceutical Engineering & Technology  
भारतीय प्रौद्योगिकी संस्थान / INDIAN INSTITUTE OF TECHNOLOGY  
(बनारस हिन्दू विश्वविद्यालय) / (BANARAS HINDU UNIVERSITY)  
वाराणसी-२२१००५ / Varanasi-221005

**Prof. S. Hemalatha**

**Head of the Department  
विभागाध्यक्ष / Head**

भैषजकीय अभियांत्रिकी एवं प्रौद्योगिकी विभाग /  
Department of Pharmaceutical Engineering & Technology  
भारतीय प्रौद्योगिकी संस्थान / INDIAN INSTITUTE OF TECHNOLOGY  
(बनारस हिन्दू विश्वविद्यालय) / (BANARAS HINDU UNIVERSITY)  
वाराणसी-२२१००५ / Varanasi-221005



**DEPARTMENT OF PHARMACEUTICAL  
ENGINEERING & TECHNOLOGY INDIAN  
INSTITUTE OF TECHNOLOGY (B. H. U.)  
VARANASI – 221005 INDIA**

---

### **COPYRIGHT TRANSFER CERTIFICATE**

**Title of the Thesis:** Preparation, phytochemical investigation and evaluation of anti-diabetic activity of polyherbal extract

**Name of the Student:** Amit Kumar Singh

### **COPYRIGHT TRANSFER**

The under signed here by assigns to the Indian Institute of Technology (Banaras Hindu University), Varanasi, all rights under copyright that may exist in and for the above thesis submitted for the award of the “*Doctor of Philosophy*”.

Date:

Place: Varanasi

*Amit Kumar Singh*

**Note:** However, the author may reproduce or authorize others to reproduce material extracted verbatim from the thesis or derivative of the thesis for author's personal use provided that the source and the Institute's copyright notice are indicated.

## LIST OF FIGURES

S. No.	Title	Page No.
1.	<b>Figure 1</b> Pathophysiology of diabetes mellitus	15
2.	<b>Figure 2</b> Medicinal plants and crude drugs of PHE.1) <i>Terminaliachebula</i> , 2) <i>Terminaliabelirica</i> , 3) <i>Andrographispaniculata</i> , 4) <i>Cyperusrotundus</i> , 5) <i>Citrulluscolocynthis</i> , 6) <i>Tinosporacardifolia</i> , 7) <i>Berberisaristata</i> , 8) <i>Nyctanthes arbor-tristis</i> , 9) <i>Premnaintegrifolia</i> , 10) <i>Picrorhizakurroa</i> , and 11) <i>Emblicoefficialis</i>	29
3.	<b>Figure 3</b> Coarse powder of ingredient medicinal plant of PHE	55
4.	<b>Figure 4</b> An illustration of the complete treatment plan and outcome of the present study	71
5.	<b>Figure 5</b> Total phenolic content, <b>A)</b> Standard gallic acid, R <sup>2</sup> values represented mean data set of n = 3 and <b>B)</b> PHE	86
6.	<b>Figure 6</b> Total flavonoid content, <b>A)</b> Standard rutin, R <sup>2</sup> values represented mean data set of n = 3 and <b>B)</b> PHE	86
7.	<b>Figure 7</b> Determination of phytochemical present in the PHE with ingredient plant extract. <b>A-D)</b> Phenol content, <b>E-F)</b> Flavonoid content (One – way analysis of variance with Tukey Post hock test, significant * p < 0.05, ** p < 0.001)	87
8.	<b>Figure 8</b> Determination of phytochemical present in the PHE with ingredient plant extract along with antioxidant potential. <b>A-B)</b> Flavonoid content, <b>C-F)</b> Antioxidant potential. (One – way analysis of variance with Tukey Post hock test, significant * p < 0.05, ** p < 0.001, *** p < 0.0001)	89
9.	<b>Figure 9</b> Determination of phytochemical present in the PHE. <b>A)</b> Phenol content, <b>B)</b> Flavonoid content, <b>C)</b> Total phenolic content, <b>D)</b> Total flavonoid content, and <b>E)</b> Antioxidant potential. (One – way analysis of variance with Tukey Post hock test)	90
10.	<b>Figure 10</b> α-Amylase inhibitory activities of PHE	93
11.	<b>Figure 11</b> α-Glucosidase inhibitory activities of PHE	94
12.	<b>Figure 12</b> Comprehensive study of anti-inflammatory and anti-diabetic activity in the PHE. <b>A)</b> Membrane stabilization, <b>B)</b> Albumin denaturation, <b>C)</b> Alpha amylase inhibition activity, <b>D)</b> Alpha glucosidase inhibition activity. (One – way analysis of variance with Tukey Post hock test)	95
13.	<b>Figure 13</b> Antihyperglycemic activity (OGTT) of PHE. (One – way analysis of variance with Tukey Post hock test), DaburMadhuRakshak (DMR)	95
14.	<b>Figure 14</b> GC-MS chromatogram of PHE	97
15.	<b>Figure 15</b> GC-MS mass peak chromatogram of Alpha-Tocospiro A	97
16.	<b>Figure 16</b> Total ion chromatogram of PHE byUPLC-Q-TOF-MS/MS	101
17.	<b>Figure 17</b> Mass data of the flavonoids identified in the UPLC-Q-TOF-MS/MS study of PHE. In positive mode <b>A)</b> Homoorientin; <b>B)</b> Puerarin; <b>C)</b> Vitexin; <b>D)</b> Eriodictyol, Acacetin, and Kaempferide; <b>E)</b> Neodiosmin and isorhamnetin-3-O-rutinoside; <b>F)</b> Diosmin	103
18.	<b>Figure 18</b> Mass data of the flavonoids identified in the UPLC-Q-TOF-MS/MS study of PHE. In negative mode <b>A)</b> Neohesperidindihydrochalcone; <b>B)</b> (+)-Catechin hydrate; <b>C)</b> syringetin-3-O-glucoside; <b>D)</b> Puerarin; <b>E)</b> Quercetin-3-Glucuronide; <b>F)</b> Luteolin-7-O-glucoside and Vitexin; <b>G)</b> Luteolin and (+-)-Taxifolin; <b>H)</b> Saponarin, Homoorientin, and Isorhamnetin-3-Galactoside-6"-Rhamnoside; <b>I)</b> Isorhamnetin-3-O-glucoside	104

19.	<b>Figure 19</b> Schematic diagram flavonoids identified in the PHE with their therapeutic values. A) Prevalent common bioactive flavonoids of PHE from UPLC-Q-TOF-MS/MS analysis; B) Puerarin; C) Homoorientin; and D) Vitexin	105
20.	<b>Figure 20</b> Total ion chromatogram of whole metabolites from PHE with relative abundance	110
21.	<b>Figure 21</b> Chebulic acid (C <sub>14</sub> H <sub>12</sub> O <sub>11</sub> ) in full scan MS of negative ionisation mode of PHE with raw, MS1 and MS2 Chromatograms	110
22.	<b>Figure 22</b> Gallic acid (C <sub>7</sub> H <sub>6</sub> O <sub>5</sub> ) in full scan MS of negative ionisation mode of PHE with raw, MS1 and MS2 Chromatograms	111
23.	<b>Figure 23</b> Andrographolide (C <sub>20</sub> H <sub>30</sub> O <sub>5</sub> ) in full scan MS of positive ionisation mode of PHE with raw, MS1 and MS2 Chromatograms	111
24.	<b>Figure 24</b> Berberine (C <sub>20</sub> H <sub>17</sub> NO <sub>4</sub> ) in full scan MS of positive ionisation mode of PHE with raw, MS1 and MS2 Chromatograms	112
25.	<b>Figure 25</b> Total ion chromatogram of whole metabolites from whole herb extract of <i>Andrographispaniculata</i>	112
26.	<b>Figure 26</b> Total ion chromatogram of whole metabolites from leaf extract of <i>Premnaintegrifolia</i>	115
27.	<b>Figure 27</b> Total ion chromatogram of whole metabolites from fruit extract of <i>Terminaliabellerica</i>	115
28.	<b>Figure 28</b> Total ion chromatogram of whole metabolites from fruit extract of <i>Terminaliachebula</i>	117
29.	<b>Figure 29</b> Total ion chromatogram of whole metabolites from stem extract of <i>Berberisaristata</i>	117
30.	<b>Figure 30</b> Total ion chromatogram of whole metabolites from leaf extract of <i>Nyctanthesarbor-tristis</i>	121
31.	<b>Figure 31</b> Stack bars with fill of anti-diabetic bioactive contents of PHE	121
32.	<b>Figure 32</b> Overlay of HPTLC chromatogram of all tracks, at wavelength with standard of kaempferol and PHE scanned at 254 nm	123
33.	<b>Figure 33</b> Overlay of HPTLC chromatogram of all tracks, at wavelength with standard of quercetin and PHE scanned at 254 nm	123
34.	<b>Figure 34</b> Overlay of HPTLC chromatogram of all tracks, at wavelength with standard of rutin and PHE scanned at 254 nm	124
35.	<b>Figure 35</b> HPTLC-images of kaempferol, quercetin, rutin and PHE scanned at 254 nm and 366 nm with standards and standard calibration plots	124
36.	<b>Figure 36</b> Images showing histology of the vital organs kidneys, heart and liver of rats treated with PHE doses. A) Control group; B) Treated dose 100mg/Kg group; C) Treated dose 200mg/Kg group; D) Treated dose 400mg/Kg group; (G: Glomerulus; BC: Bowman's capsule; GS: Glomerular space; PL: Parietal layer; VL: Visceral layer; MF: Cardiac muscle fibers; MFV: Cardiac muscle fiber vacuolation; CV: Central vein; HP: Hepatocytes; HS: Hepatic sinusoids and HC: Hepatic cord)	132
37.	<b>Figure 37</b> Images showing histology of the lung, spleen, pancreas and brain of rats treated with PHE doses. A) Control group; B) Treated dose 100mg/Kg group; C) Treated dose 200mg/Kg group; D) Treated dose 400mg/Kg group; (A: Alveoli; B: Bronchiole; LF: Lymphoid follicles; GL: Granular leukocytes; S: Sinusoids; CAC: Centroacinar cells; ILD: Intralobular duct; PA: Pancreatic acini; PL: Pancreatic lobule; PC: Pyramidal cells; GC: Glial cells; BV: Blood vessels and V: Vacuolization)	133

38. **Figure 38** OGTT blood glucose levels of streptozotacin-induced diabetic rats after oral administration of PHE. Data are expressed as mean  $\pm$  SEM ( $n = 6$ ). \*\*\* Statistically significant ( $p < 0.0001$ ) between diabetic to treatment group. PHE: Poly herbal extract; DMR: daburmadhurakshak 134
39. **Figure 39** Anti-diabetic effect of PHE on body weight. Data are expressed as mean  $\pm$  SEM ( $n = 6$ ). \*Statistically significant ( $p < 0.05$ ) to diabetic control; # statistically significant ( $p < 0.05$ ) to normal; \*\*  $P < 0.01$  is considered as very significant. 135
40. **Figure 40** Anti-diabetic effect of PHE on fasting blood glucose level. Data are expressed as mean  $\pm$  SEM ( $n = 6$ ). \*Statistically significant ( $p < 0.05$ ) to DC; # statistically significant ( $p < 0.05$ ) to NC; ##  $P < 0.01$  is considered as very significant. PHE: Poly herbal extract; DMR: daburmadhurakshak 136
41. **Figure 41** The anti-diabetic effects of PHE on *in-vivo* diabetic-parameters of streptozotacin-induced diabetic rats. **A)** HbA1C, **B)** Insulin, **C)** HOMA- $\beta$  cells, **D)** HOMA-IR, **E)** ALT, **F)** AST, **G)** ALP, **H)** TP, **I)** UA, **J)** CRE, **K)** BUN levels, **L)** Total cholesterol, and **M)** Triglyceride. Data are expressed as mean  $\pm$  SEM ( $n = 6$ ). \*Statistically significant ( $p < 0.05$ ) to DC; # statistically significant ( $p < 0.05$ ) to NC. PHE: Poly herbal extract; DMR: daburmadhurakshak; HbA1c: hemoglobin A1c (glycated hemoglobin); HOMA-IR: homeostatic model assessment of insulin resistance; HOMA- $\beta$ : homeostatic model assessment of  $\beta$ -cell function; ALT: alanine transaminase; AST: aspartate aminotransferase; ALP: alkaline phosphatase; TP: total protein; UA: uric acid; CRE: creatinine; BUN: blood urea nitrogen. 137
42. **Figure 42** The effects of PHE on lipid metabolism parameters, antioxidant, anti-inflammatory, and apoptotic markers in the hepatic as well as pancreatic tissues of streptozotacin-induced diabetic rats. **A)** LDL, **B)** VLDL, **C)** HDL, **D)** Hepatic CAT, **E)** Hepatic GSH, **F)** Hepatic SOD, **G)** Hepatic MDA, **H)** Pancreatic CAT, **I)** Pancreatic GSH, **J)** Pancreatic SOD, **K)** Pancreatic MDA levels, **L)** Hepatic TNF, **M)** Hepatic Bcl-2, **N)** Pancreatic Bcl-2, and **O)** Pancreatic TNF. Data are expressed as mean  $\pm$  SEM ( $n = 6$ ). \*Statistically significant ( $p < 0.05$ ) to DC; # statistically significant ( $p < 0.05$ ) to NC. PHE: Poly herbal extract; DMR: daburmadhurakshak; TC: total cholesterol; TG: triglyceride; HDL: high density lipoprotein; VLDL: very low density lipoprotein; LDL: low density lipoprotein-cholesterol; CAT: catalase; SOD: superoxide dismutase; GSH: reduced glutathione; MDA: malondialdehyde. 138
43. **Figure 43** The effects of PHE on anti-inflammatory, and apoptotic markers in the hepatic as well as pancreatic tissues of streptozotacin-induced diabetic rats. **A)** Hepatic COX-2, **B)** Hepatic IL-18, **C)** Hepatic IL-4, **D)** Hepatic SOX-9, **E)** Pancreatic IL-4, **F)** Pancreatic COX-2, **G)** Pancreatic IL-18, **H)** Pancreatic SOX-9. Data are expressed as mean  $\pm$  SEM ( $n = 6$ ). \*Statistically significant ( $p < 0.05$ ) to DC; # statistically significant ( $p < 0.05$ ) to NC. 140
44. **Figure 44** Light microscopic pictures of pancreas sections for TNF immunostaining (brown-red color; H&E x100). **A)** Normal control group showing normal structure of the Islets of Langerhans and acini; **B)** Diabetic control group showing degeneration of the islet; **C)** Diabetic + metformin treated group showing preservation of the architectural structure of Islet of Langerhans; **D)** Diabetic + PHE 300 mg/kg treated group showing restoration of the architectural structure of Islet of Langerhans; **E)** Diabetic + PHE 600 mg/kg treated group showing restoration of the architectural structure of Islet of Langerhans, acini; **F)** Diabetic + 142

- DMR treated group showing partial restoration of the architectural structure of Islet of Langerhans; **G**) TNF positive cells of streptozotacin-induced diabetic rats after oral administration of PHE. Data are expressed as mean  $\pm$  SEM (n = 6).
45. **Figure 45** Light microscopic pictures of pancreas sections for COX-2 immunostaining (brown-red color; H&E x100). **A**) Normal control group showing normal structure of the Islets of Langerhans and acini; **B**) Diabetic control group showing degeneration of the islet; **C**) Diabetic + metformin treated group showing preservation of the architectural structure of Islet of Langerhans; **D**) Diabetic + PHE 300 mg/kg treated group showing restoration of the architectural structure of Islet of Langerhans; **E**) Diabetic + PHE 600 mg/kg treated group showing restoration of the architectural structure of Islet of Langerhans, acini; **F**) Diabetic + DMR treated group showing partial restoration of the architectural structure of Islet of Langerhans; **G**) COX-2 positive cells of streptozotacin-induced diabetic rats after oral administration of PHE. Data are expressed as mean  $\pm$  SEM (n = 6). 143
46. **Figure 46** Light microscopic pictures of pancreas sections for IL-18 immunostaining (brown-red color; H&E x100). **A**) Normal control group showing normal structure of the Islets of Langerhans and acini; **B**) Diabetic control group showing degeneration of the islet; **C**) Diabetic + metformin treated group showing preservation of the architectural structure of Islet of Langerhans; **D**) Diabetic + PHE 300 mg/kg treated group showing restoration of the architectural structure of Islet of Langerhans; **E**) Diabetic + PHE 600 mg/kg treated group showing restoration of the architectural structure of Islet of Langerhans, acini; **F**) Diabetic + DMR treated group showing partial restoration of the architectural structure of Islet of Langerhans; **G**) IL-18 positive cells of streptozotacin-induced diabetic rats after oral administration of PHE. Data are expressed as mean  $\pm$  SEM (n = 6). 144
47. **Figure 47** Light microscopic pictures of pancreas sections for SOX-9 immunostaining (brown-red color; H&E x100). **A**) Normal control group showing normal structure of the Islets of Langerhans and acini; **B**) Diabetic control group showing degeneration of the islet; **C**) Diabetic + metformin treated group showing preservation of the architectural structure of Islet of Langerhans; **D**) Diabetic + PHE 300 mg/kg treated group showing restoration of the architectural structure of Islet of Langerhans; **E**) Diabetic + PHE 600 mg/kg treated group showing restoration of the architectural structure of Islet of Langerhans, acini; **F**) Diabetic + DMR treated group showing partial restoration of the architectural structure of Islet of Langerhans; **G**) SOX-9 positive cells of streptozotacin-induced diabetic rats after oral administration of PHE. Data are expressed as mean  $\pm$  SEM (n = 6). 145
48. **Figure 48** Light microscopic pictures of pancreas sections for IL-4 immunostaining (brown-red color; H&E x100). **A**) Normal control group showing normal structure of the Islets of Langerhans and acini; **B**) Diabetic control group showing degeneration of the islet; **C**) Diabetic + metformin treated group showing preservation of the architectural structure of Islet of Langerhans; **D**) Diabetic + PHE 300 mg/kg treated group showing restoration of the architectural structure of Islet of Langerhans; **E**) Diabetic + PHE 600 mg/kg treated group showing restoration of the architectural structure of Islet of Langerhans, acini; **F**) Diabetic + DMR treated group showing partial restoration of the architectural structure of Islet of Langerhans; **G**) IL-4 positive cells of streptozotacin-induced diabetic rats after oral administration of PHE. Data are expressed as mean  $\pm$  SEM (n = 6). 146

49. **Figure 49** Light microscopic pictures of pancreas sections for Bcl-2 immunostaining (brown-red color; H&E x100). **A)** Normal control group showing normal structure of the Islets of Langerhans and acini; **B)** Diabetic control group showing degeneration of the islet; **C)** Diabetic + metformin treated group showing preservation of the architectural structure of Islet of Langerhans; **D)** Diabetic + PHE 300 mg/kg treated group showing restoration of the architectural structure of Islet of Langerhans; **E)** Diabetic + PHE 600 mg/kg treated group showing restoration of the architectural structure of Islet of Langerhans, acini; **F)** Diabetic + DMR treated group showing partial restoration of the architectural structure of Islet of Langerhans; **G)** Bcl-2 positive cells of streptozotacin-induced diabetic rats after oral administration of PHE. Data are expressed as mean  $\pm$  SEM (n = 6). 147
50. **Figure 50** Histogram of Sequence reads. **A)** Per sequence quality score and **B)** Mean quality score. 148
51. **Figure 51** Histogram of sequence diversity; **(A)** Contig length distribution and **(B)** Gel Image showing the amplicon size along with 100bp ladder. 149
52. **Figure 52** Rarefaction curve of sequence diversity GP1 (Normal), GP2 (Diabetic Control), GP3 (Metformin), GP4 (PHE 300 mg/kg), GP5 (PHE 600 mg/kg), and GP6 (DMR). 150
53. **Figure 53** Alpha diversity measurement of gut microbiomes for different treatment groups 153
54. **Figure 54** The taxonomic composition relative abundance of gut microbial in rat fecal sample of different experimental (GP-1 to GP-6) groups (n = 6). **(A)** PCoA plot, **(B)** Phylum level, **(C)** Genus level and **(D)** Species level 154
55. **Figure 55** The taxonomic composition with relative abundance heat map of gut microbial in rat fecal sample of different experimental (GP-1 to GP-6) groups (n = 6). **(A)** Phylum level, **(B)** Genus level and **(C)** Species level 158
56. **Figure 56** Correlation analysis between DM-related parameters (body weight and FBG) and gut microbiota at genus level. Canonical correspondence analysis **(A)** Body weight Vs gut microbiota and **(B)** FBG Vs gut microbiota 159
57. **Figure 57** SCFAs analysis in the fecal sample of different rat groups. **A)** Standard graph of acetic acid (with  $R^2 = 0.998$ ) and **B)** propionic acid (with  $R^2 = 0.996$ ). **C)** The concentration of acetic acid, **D)** The concentration of propionic acid 161
58. **Figure 58** Krona-pie-charts of gut microbiota structures at family level. **A)** Normal rats with 6% Prevotellaceae, **B)** Diabetic control rats with 0.2% Prevotellaceae, **C)** Metformin group rats with 4% Prevotellaceae, **D)** 300 mg/kg PHE-treated rats with 0.2% Prevotellaceae, **E)** 600 mg/kg PHE-treated rats with 7% Prevotellaceae, and **F)** DMR-treated rats with 4% Prevotellaceae 163
59. **Figure 59** Canonical correlation analysis (CCA) between gut microbiota and lipid metabolism indexes performed through XLSTAT 2023.1.2.1406 164
60. **Figure 60** Potential active ingredients of PHE, core targets identification and network construction for the treatment of DM. **A)** ADMET score of all the compounds to have drug like property, **B)** Potential 331 core targets identification between 675 STP genes related to all compounds and 2803 DisGenet genes related to DM, **C)** Potential 57 core targets identification between 105 STP genes related to ATA compound and 2803 DisGenet genes related to DM, **D)** PPI network of PHE, and **E)** Compound target network of PHE with top selected genes, light blue diamond shapes represent core compounds and yellow squares represent important potential targets 166

61.	<b>Figure 61</b> Network construction, hub gene analysis, functional annotation and potential molecular pathways of ATA for the treatment of DM. <b>A)</b> PPI network of ATA, <b>B)</b> Compound target disease network of ATA, green square represents important potential core compound-ATA, pink rectangles represent important potential targets and red square represents DM. <b>C)</b> Top 13 selected hub genes network of ATA, <b>D)</b> Molecular functions, <b>E)</b> Biological processes, <b>F)</b> Cellular components, <b>G)</b> Top most KEGG pathway enrichment in study of ATA	173
62.	<b>Figure 62</b> KEGG pathway enrichment, heat map of PASS activity and molecular docking diagram of the ATA with key targets. <b>A)</b> TNF as hub signaling pathway from KEGG pathway enrichment, <b>B)</b> Heat map of top probable bioactivities in the PASS study, <b>C)</b> 3D interaction diagram with AKT1, <b>D)</b> 2D interaction diagram with AKT1, <b>E)</b> 3D interaction diagram with TNF, <b>F)</b> 2D interaction diagram with TNF	174
63.	<b>Figure 63</b> Interaction of Alpha Tocospiro A with TNF- $\alpha$ chain-C, <b>A)</b> 3D and <b>B)</b> 2D	180
64.	<b>Figure 64</b> Interaction of Alpha Tocospiro A with TNF- $\alpha$ chain-A, <b>A)</b> 3D and <b>B)</b> 2D	180
65.	<b>Figure 65</b> Common potential targets of biomarker compounds of PHE against DM	183
66.	<b>Figure 66</b> The PPI network for common targets of biomarker compounds and DM	183
67.	<b>Figure 67</b> The 249 core targets of biomarker compounds of PHE against DM	184
68.	<b>Figure 68</b> The top 10 hub targets of biomarker compounds of PHE against DM	184
69.	<b>Figure 69</b> <b>A)</b> Prominent signaling pathway involve in KEGG analysis and <b>B)</b> biological processes of GO analysis for biomarker compounds of PHE against DM	185
70.	<b>Figure 70</b> <b>A)</b> Cellular component and <b>B)</b> molecular function of GO analysis for biomarker compounds of PHE against DM	186
71.	<b>Figure 71</b> 3D and 2D interaction images of apigenin against the DM-related target TP53	189
72.	<b>Figure 72</b> 3D and 2D interaction images of berberine against the DM-related target IL4	189
73.	<b>Figure 73</b> 3D and 2D interaction images of berberine against the DM-related target TNF	190
74.	<b>Figure 74</b> Heat maps of gut microbiota structures. <b>A)</b> Heat map of gut microbiota structures of all group rats at genus level, <b>B)</b> Cluster auto polar heat map of gut microbiota-family with enrichment of Prevotellaceae and Ruminococcaceae in the treatment groups. Gut microbiota-metabolite-target network. <b>C)</b> Lactobacillus, <b>D)</b> Prevotella, <b>E)</b> Clostridium, <b>F)</b> Ruminococcus, and <b>G)</b> Bacteroides.	194
75.	<b>Figure 75</b> Venny overlapping images, PPI network, KEGG and gene ontology study of key targets in the present study. <b>A)</b> Identification of 266 key targets of all metabolites, <b>B)</b> 2352 Common targets of DM related genes, <b>C)</b> 132 key targets of metabolites and DM related genes, <b>D)</b> PPI network of 8 core target genes through String web server, <b>E)</b> Identification of enrichment of KEGG pathways through ShinyGo database, and <b>F)</b> Dotplot for 3 Functional component of core targets in gene ontology study.	195
76.	<b>Figure 76</b> Enrichment of the core genes in KEGG AGE-RAGE signaling pathway in diabetic complications	196
77.	<b>Figure 77</b> The molecular docking test on core targets of AGE-RAGE signaling pathway in diabetic complications and TNF signaling pathways with metabolites of gut microbiota. <b>A)</b> Ursodeoxycholic acid-MMP2 (PDB ID: 3AYU), <b>B)</b> Ursodeoxycholic acid-CASP3 (PDB ID: 4JQZ) and <b>C)</b> Ursodeoxycholic acid-MMP14 (PDB ID: 4QXU).	199

---

## LIST OF TABLES

S. No.	Title	Page No.
1.	<b>Table 1</b> Taxonomic classification, common name, phyto-chemical, uses, and therapeutic benefits of ingredient medicinal plants of PHE	25
2.	<b>Table 2</b> Design of 4 different poly herbal combinations containing 6 medicinal plants each	58
3.	<b>Table 3</b> Microwave digestion program for the digestion of PHE sample	59
4.	<b>Table 4</b> Operating conditions for ICP-MS determination of Pb, Cd, As, Hg and Ni in digested sample	59
5.	<b>Table 5</b> Parameters of HPTLC for quantification of quercetin, rutin and kaempferol in the PHE	66
6.	<b>Table 6</b> The antisense and sense mRNA sequences (5'→3') of the primers for RT-PCR	75
7.	<b>Table 7</b> Plant name, part used and percent yield of PHE	85
8.	<b>Table 8</b> Antioxidant potential of all formulation and standard in the study	88
9.	<b>Table 9</b> Concentration of heavy metals (Pb, Cd, As, Hg and Ni by ICP-MS) determination of PHE	91
10.	<b>Table 10</b> Mean data of heavy metals Pb, Cd, As, Hg and Ni in ICP-MS determination of PHE	91
11.	<b>Table 11</b> <i>In vitro</i> anti-inflammatory study of PHE	92
12.	<b>Table 12</b> $\alpha$ -Amylase inhibitory activities of PHE	93
13.	<b>Table 13</b> $\alpha$ -Glucosidase inhibitory activities of PHE.	94
14.	<b>Table 14</b> Determination of IC <sub>50</sub> for the PHE	94
15.	<b>Table 15</b> GC-MS fingerprint of PHE	99-100
16.	<b>Table 16</b> Phytochemical analysis of PHE by UPLC-Q-TOF-MS/MS	102
17.	<b>Table 17</b> Flavonoids identified in UPLC-Q-TOF-MS/MS study of PHE	106
18.	<b>Table 18</b> UHPLC-HRAMSS-based metabolic profile of PHE	109
19.	<b>Table 19</b> UHPLC-HRAMSS-based metabolic profile of whole herb extract of <i>Andrographis paniculata</i>	113
20.	<b>Table 20</b> UHPLC-HRAMSS-based metabolic profile of leaf extract of <i>Premna integrifolia</i>	114
21.	<b>Table 21</b> UHPLC-HRAMSS-based metabolic profile of fruit extract of <i>Terminalia bellerica</i>	116
22.	<b>Table 22</b> UHPLC-HRAMSS-based metabolic profile of fruit extract of <i>Terminalia chebula</i>	118
23.	<b>Table 23</b> UHPLC-HRAMSS-based metabolic profile of stem extract of <i>Berberis aristata</i>	119
24.	<b>Table 24</b> UHPLC-HRAMSS-based metabolic profile of leaf extract of <i>Nyctanthes arbor-tristis</i>	120
25.	<b>Table 25</b> Weight of rat treated with PHE	125
26.	<b>Table 26</b> Relative organ weight (gm/150gm) of rat treated with PHE	125
27.	<b>Table 27</b> Erythrogram, leukogram and platelet count of rats treated with PHE	126
28.	<b>Table 28</b> Biochemical parameters of rats treated with single dose of PHE	127

29.	<b>Table 29</b> Body weight of rats treated with repeated doses of PHE	129
30.	<b>Table 30</b> Relative organ weight (gm/150gm) treated with repeated doses of PHE	129
31.	<b>Table 31</b> Erythrogram, leukogram and platelet count treated with repeated doses of PHE	130
32.	<b>Table 32</b> Biochemical parameters treated orally with repeated doses of PHE	131
33.	<b>Table 33</b> Body weight of streptozotacin-induced diabetic rats before and after oral administration of PHE	135
34.	<b>Table 34</b> Summary of raw sequence data and quality checks	149
35.	<b>Table 35</b> Alpha diversity measurement of gut microbiota for different treatment groups	151
36.	<b>Table 36</b> HPLC-based estimation of standard SCFAs	161
37.	<b>Table 37</b> Gut microbiota (%) diversity at family level	162
38.	<b>Table 38</b> Gut microbiota (%) abundance at genus level	164
39.	<b>Table 39</b> ADMET score of all compounds of PHE.	167
40.	<b>Table 40</b> Degree value of top genes related to PHE in network	169
41.	<b>Table 41</b> Degree value of compounds of PHE in network	170
42.	<b>Table 42</b> Target genes of KEGG pathways enrichment analysis of ATA related to DM	175
43.	<b>Table 43</b> Pass predicted bioactivity of Alpha Tocospiro A	178
44.	<b>Table 44</b> The docking results (binding energy) of ligand (Alpha Tocospiro A) and the hub genes (AKT1 and TNF- $\alpha$ ) along their respective number of hydrogen bonds as well as interacting amino acids related to DM	179
45.	<b>Table 45</b> ADMET and drug-like properties of biomarker compounds of PHE	181
46.	<b>Table 46</b> Molecular docking test results of biomarker compounds of PHE and high scoring DM-related targets	187
47.	<b>Table 47</b> Molecular docking test information of biomarker compounds of PHE and high scoring DM-related targets	188
48.	<b>Table 48</b> Gut metabolites and their potential target genes through gutMgene database	191-192
49.	<b>Table 49</b> Target genes network-score through STRING sever	192
50.	<b>Table 50</b> Overlapping target genes of human genome within direct network and their score through STRING sever	193
51.	<b>Table 51</b> Binding affinity score of metabolites for the core target genes	198

---

## LIST OF ABBREVIATIONS

Abbreviation: Full name	Abbreviation: Full name
<b>AGEs:</b> Advanced glycation end products	<b>ICP-MS:</b> Inductively Coupled Plasma Mass Spectrometry
<b>ALP:</b> Alkaline phosphatase	<b>IHC:</b> Immuno Histochemistry
<b>ALT:</b> Alanine transaminase	<b>KEGG:</b> Kyoto Encyclopedia of Genes and Genomes
<b>AP:</b> <i>Andrographispaniculata</i> Nees.	<b>KM:</b> Kaempferol
<b>As:</b> Arsenic	<b>LC-MS:</b> Liquid chromatography-mass spectroscopy
<b>AST:</b> Aspartate aminotransferase	<b>LDL:</b> Low-density lipoprotein
<b>ATA:</b> Alpha Aocospiro A	<b>MDA:</b> Malondialdehyde
<b>BA:</b> <i>Berberisaristata</i> DC.	<b>MDT:</b> Molecular Docking Test
<b>Bcl-2:</b> B-Cell Lymphoma 2	<b>META:</b> Metabolite
<b>BF:</b> Biological Function	<b>MF:</b> Molecular Function
<b>BMI:</b> Body mass index	<b>MODY:</b> Maturity onset diabetes of the young
<b>BP:</b> Biological process	<b>NA:</b> <i>Nyctanthesarbortristis</i> L.
<b>BQL:</b> Below the quantification limit	<b>Ni:</b> Nickel
<b>BUN:</b> Blood urea nitrogen	<b>OGTT:</b> Oral Glucose Tolerance Test
<b>CAT:</b> Catalase	<b>OUT:</b> Operational taxonomic unit
<b>CBC:</b> Complete blood count	<b>Pb:</b> Lead
<b>CC:</b> Cellular Component	<b>PHE:</b> Poly Herbal Extract
<b>CCA:</b> Canonical correspondence analysis	<b>PI:</b> <i>Premnaintegrifolia</i> L.
<b>Cd:</b> Cadmium	<b>PPI:</b> Protein-Protein Interaction
<b>CRE:</b> Creatinine	<b>QCT:</b> Quercetin
<b>DM:</b> Diabetes mellitus	<b>RE:</b> Rutin equivalent
<b>DMR:</b> Dabar Madhu Rakshak	<b>ROS:</b> Reactive oxygen species
<b>DMR:</b> Dabur Madhu Rakshak	<b>RT:</b> Retention time, Rutin
<b>DMSO:</b> Dimethylsulfoxide	<b>SCFA:</b> Short Chain Fatty Acid
<b>DNSA:</b> 3,5 Dinitro Salicylic Acid	<b>SEA:</b> Similarity Ensemble Approach
<b>DPP-IV:</b> Dipeptidyl peptidase IV	<b>SGLT2:</b> Sodium-glucose transport protein 2
<b>FBG:</b> Fasting Blood Glucose	<b>SOD:</b> Superoxide Dismutase
<b>GAE:</b> Gallic acid equivalent	<b>STP:</b> Swiss Target Prediction
<b>GC-MS:</b> Gas chromatography-mass spectroscopy	<b>STP:</b> Swiss Target Prediction
<b>GLP-1:</b> Glucagon-like peptide 1	<b>STZ:</b> Streptozotocin
<b>GLUT:</b> Glucose transporter	<b>STZ:</b> Streptozotocin
<b>GM:</b> Gut Microbiota	<b>T1DM:</b> Type 1 Diabetes mellitus
<b>GO:</b> Gene Ontology	<b>T2DM:</b> Type 2 Diabetes mellitus
<b>GSH:</b> Glutathione peroxidase (reduced glutathione)	<b>TB:</b> <i>Terminaliabellerica</i> Roxb.
<b>GSK3:</b> Glycogen synthase kinase 3	<b>TC:</b> <i>Terminaliachebula</i> Retz., Total cholesterol
<b>HbA1c:</b> Glycated hemoglobin	<b>TCMSP:</b> Traditional Chinese Medicine Systems Pharmacology
<b>HbA1c:</b> Hemoglobin A1C	<b>TFC:</b> Total flavonoid content

**HDL:** High density lipoprotein

**Hg:** Mercury

**HNF1 $\alpha$ :** Hepatocyte nuclear factor 1  $\alpha$

**HOMA-IR:** Homeostasis Model Assessment of Insulin Resistance

**HOMA- $\beta$ :** Homeostasis Model Assessment of  $\beta$ -Cell Function

**HPLC:** High-performance liquid chromatography

**HPTLC:** High Performance Thin Layer Chromatography

**HRMS:** High-resolution mass spectroscopy

**TG:** Target Gene, Triglyceride

**TLC:** Thin Layer Chromatography

**TNF- $\alpha$ :** Tumor Necrosis Factor- $\alpha$

**TP:** Total protein

**TPC:** Total phenolic content

**UA:** Uric acid

**UDCA:** Ursodeoxycholic acid

**VLDL:** Very low density lipoprotein

---

## PREFACE

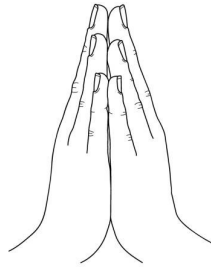
---

This thesis on “Preparation, phytochemical investigation and evaluation of anti-diabetic activity of polyherbal extract” aims at giving an insight at various aspects of the chronic disease named as diabetes mellitus and the risk factors that lead to it; the various ways it develops in the human body; the old and new approaches to treatment, both from a pharmacological and a computational (bioinformatics approach) point of view; ways to prevent and to manage the diabetes complications; how to improve the lives of the diabetic patients who are faced with not only physical but also psychological problems; statistical data from around the world which focuses on epidemiology and outlines the issue of the cost of diabetes. The entire thesis work has been divided into nine chapters, which fulfill four objectives as follows:

**Chapter 1** deals with the general introduction to diabetes mellitus and its relation to oxidative stress and antidiabetic activity of medicinal plants, the phytochemical composition of polyherbal extracts (polyphenols, flavonoids, and others), gut microbiota dysbiosis, and the enrichment of beneficial short-chain fatty acids through the gut microbiome. It also covers the general strategy adopted for antidiabetic activity and highlights the motivations and significance of research work. The objectives of the thesis work are also part of Chapter 1. **Chapter 2** presents the literature survey covering strategies for selection of medicinal plants with antidiabetic activity, extraction, purification, and characterization of phytochemicals. It also covers the classification of polyphenols and flavonoids related to diabetic management and therapeutic applications. **Chapter 3** describes the research objectives and plan of work, which include step-by-step differentiation of the work.

**Chapter 4** presents materials and methods adapted to perform this work. This includes various techniques involved in extraction, purification, and characterization. *In vitro* and *in silico* evaluation of phytochemicals from polyherbal extract (PHE) as an antidiabetic agent and antidiabetic activity evaluation through gut microbiota eubiosis by phytochemical gut microbiota metabolite brain axis. **Chapter 5** deals with all the results of *in vitro*, *in silico*, and *in vivo* studies of PHE with the involvement of short-chain fatty acids through beneficial gut microbiota enrichment. **Chapter 6** presents the discussion of the whole studies with phytochemicals like polyphenols and flavonoids and the evaluation of the antioxidant potential of these through antidiabetic activity in traditional ways as well as in a newer way with the eubiosis of gut microbiota. **Chapter 7** deals with the conclusion of the whole study, which focuses mainly on the antidiabetic evaluation of PHE through various approaches. **Chapter 8** deals with future aspects of the study involving clinical trial studies on human volunteers. **Chapter 9** presents a brief overview of publications during the experimental work and findings.

Finally, our study strengthened the possibility that PHE and possibly gut microbiota metabolites from this investigation could one day be novel medications and approaches in the field of pharmacological intervention for diabetes. When taken as a whole, the encouraging PHE reported in this study may prove to be a lead medication option in the future that helps with diabetes management.



**DEDICATED**  
**TO**  
**MY TEACHERS**  
**AND BELOVED**  
**FAMILY MEMBERS**